

# Majorana phase-gate based on the geometric phase

Andrzej Więckowski,<sup>\*</sup> Marcin Mierzejewski,<sup>†</sup> and Michał Kupczyński<sup>‡</sup>  
Department of Theoretical Physics, Faculty of Fundamental Problems of Technology,  
Wrocław University of Science and Technology, PL-50370 Wrocław, Poland

We study dynamics of a single qubit encoded in two pairs of Majorana modes, whereby each pair is hosted on a trijunction described by the Kitaev model extended by many-body interactions. We demonstrated that the challenging phase-gate may be efficiently implemented via braiding of partially overlapping modes. Although such qubit acquires both geometric and dynamical phases during the braiding protocol, the latter phase may be eliminated if the Majorana modes are hosted by systems with appropriate particle-hole symmetry.

## I. INTRODUCTION

The Majorana zero-energy modes (MZMs) have recently attracted a significant interest as building blocks of the future topological quantum computers [1–11]. So far, the experimental and theoretical studies have focused mostly on finding an optimal physical system that hosts the MZM [12–18] as well as on developing appropriate techniques which clearly confirm the existence of MZM therein [19–21]. Recent experimental results strongly support the presence of the MZM in superconductor–semiconductor hybrid nanostructures [22–31], in one-dimensional monoatomic chains deposited on the surface of superconductors [32–37], in the superconducting vortices [38–41] and in two-dimensional topological superconductors [42, 43].

The fundamental problem for quantum computing is to effectively implement the set of the universal gates which consists of the Hadamard gate, the Z gate and also the  $\pi/8$ -gate (phase-gate) [44]. The general scheme for building the former two gates is already well established via topologically protected braiding operations of MZMs [45–56]. However, the phase-gate poses a challenging problem, since the latter operations are insufficient for its implementation [6]. The very basic method of overcoming this problem is to bring two Majorana quasiparticles close to each other [6]. The MZMs are operators which map an eigenstate from one parity sector to a state in another sector with identical energy. Bringing two MZMs together lifts the latter degeneracy (MZMs are no longer strict zero-modes) and splits the levels for odd and even numbers of particles by  $\delta E$ . In principle, the phase-shift needed for the phase-gate can be obtained via fine-tuning of two parameters:  $\delta E$  and the period of time  $\Delta t$  for which the MZMs are brought close to each other. However, the resulting phase is not protected by any symmetry and, as a consequence, each such operation must be followed by an error correction, e.g. via the magic state distillation [57].

The phase-shift induced via proximity of two MZMs is a dynamical phase. Such operation requires a precise control of two independent parameters:  $\delta E$  and  $\Delta t$ . In the present work we derive other possibility in which fine-tuning of  $\Delta t$  is eliminated. It consists in double braiding of two MZMs, which are

previously brought together, so that the Majorana edge states partially overlap in the real space. Braiding of such overlapping modes leads to a small shift of the *geometric phase* with respect to results for spatially separated MZMs [53]. The geometric phase is independent of the braiding time,  $\Delta t$ , hence it is better suited building of the phase-gate than simple protocol based on the dynamical phase. Despite an apparent advantage of such protocol, an important problem remains to be solved: qubit built out of overlapping MZMs acquires during its evolution not only the geometric but also the dynamical phase, whereby the latter occurs due to the energy splitting  $\delta E$ . However, we demonstrate that the dynamical phase may be effectively eliminated if the MZMs are hosted by appropriate systems with particle–hole symmetry. The latter property is shown to hold also for systems with many-body interactions.

The paper is organized as follows: in Section II we recall the method of storing a qubit in 4 MZM (sparse encoding) and specify the microscopic model of a system that hosts MZMs; next, in Section III we present our numerical results concerning the geometric- and dynamical-phases gained after the braiding of overlapping Majorana modes and show how the latter phase may be eliminated; finally, we summarize our results in Section IV.

## II. MODEL AND DETAILS OF BRAIDING

We study the dynamics of a single qubit (sparsely) encoded in two pairs of MZMs,  $\Gamma_1, \Gamma_2$  and  $\Gamma_3, \Gamma_4$ . Each pair of MZMs is hosted on a trijunction schematically shown in Fig. 1(a). The basis of the qubit consists of two states with even total number of fermions,  $|0\rangle = |e_{12}\rangle \otimes |e_{34}\rangle$  and  $|1\rangle = |o_{12}\rangle \otimes |o_{34}\rangle$ . Here,  $|e_{12}\rangle$  and  $|o_{12}\rangle$  denote the states of the junction  $J_{12}$  with even and odd number of fermions, respectively. Similar notation holds for junction  $J_{34}$ .

We study the simplest setup which allows for the braiding of MZMs [45, 53]. Namely, we consider a trijunction [cf. Fig. 1(a)] consisting of three chains of equal length and we set for each chain different phase of the superconducting order parameter,  $\Delta_{ij} = \Delta \exp(-i\phi_{ij})$ , where  $\phi_{ij} = 0, +\frac{\pi}{2}, -\frac{\pi}{2}$  in left, right and the vertical chain, respectively. We assume also that each junction contains  $L$  sites and is described by the Kitaev

<sup>\*</sup> andrzej.wieckowski@pwr.edu.pl

<sup>†</sup> marcin.mierzejewski@pwr.edu.pl

<sup>‡</sup> michal.kupczynski@pwr.edu.pl

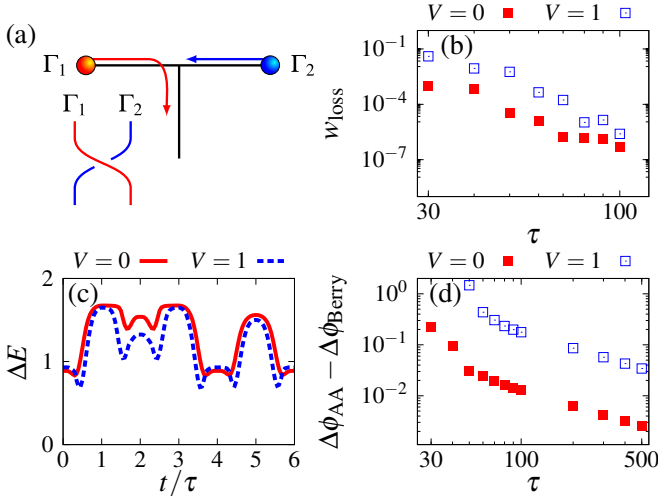


FIG. 1. (a) Sketch of trijunction hosting a pair of MZMs,  $\Gamma_1$  and  $\Gamma_2$ , as well as the braiding procedure marked schematically with arrows; (b) loss of the fidelity,  $w_{\text{loss}}$ , as a function of the total evolution-time  $T = 6\tau$ ; (c) energy gap  $\Delta E$  vs. time  $t/\tau$ ; (d) difference between  $\Delta\phi_{\text{AA}}$  and  $\Delta\phi_{\text{Berry}}$  vs. the evolution time  $T = 6\tau$ . Results for system with ( $V = 1$ ) and without ( $V = 0$ ) many-body interactions (see labels) for  $L = 7$ ,  $\Delta = 0.8$ ,  $\mu = 0$ .

model [58] with many-body interaction [59–65],

$$H(t) = H_0 + \sum_i \mu_i(t) \tilde{n}_i, \quad (1)$$

$$H_0 = \sum_{\langle i,j \rangle} \left[ (t_0 a_i^\dagger a_j + \Delta_{ij} a_i^\dagger a_j^\dagger) + \text{H.c.} + V \tilde{n}_i \tilde{n}_j \right].$$

Here  $a_i^\dagger$  creates a fermion on site  $i$ ,  $\tilde{n}_i = a_i^\dagger a_i - \frac{1}{2}$ ,  $t_0$  is the hopping between the neighboring sites on a junction,  $V$  is the nearest neighbor repulsion. The time-dependence of  $\mu_i(t)$  allows to implement the braiding of MZMs as it is described below in more details. We use dimensionless units,  $\hbar = 1$  and  $t_0 = 1$ .

In the case of a single Kitaev chain with a uniform and time-independent  $\mu_i(t) = \mu$ , one may switch between the trivial and the topological phases via tuning the chemical potential. In a system without many-body interaction ( $V = 0$ ) and non-zero  $|\Delta| > 0$ , the topological phase is present for  $|\mu| \leq 2t_0$ , while the trivial one for  $|\mu| > 2t_0$  [58, 66]. The topological regime in a system with many-body interaction has been discussed, e.g., in [59, 60, 67]. The braiding is achieved via slow tuning of  $\mu_i(t)$  in such a way that selected sites remain in topological regime whereas the other remain in the trivial regime [45]. Namely,

$$\mu_i(t) = \mu_c g_i(t) + \mu, \quad (2)$$

where  $\mu$  is the uniform chemical potential and we set  $\mu_c = \pm 4$ . The details of the ramping protocol,  $g_i(t) \in [0, 1]$ , are the same as in Ref. [53] and are recalled in the Appendix A.

The braiding protocol describes a cyclic evolution of the Hamiltonian (1) in the parameter space. The many-body wave function is obtained from the numerical solution [68, 69] of the time-dependent Schrödinger equation  $i\partial_t |\psi(t)\rangle =$

$H(t)|\psi(t)\rangle$ . Initially ( $t = 0$ ), we set  $\mu_i = \mu_c$  for sites  $i$  in the vertical chain [cf. Fig. 1(a)] which is then in the trivial regime. Two remaining (horizontal) chains are in topological regime and host two MZMs located at the edges of these wires. Next, by adiabatic tuning of  $g_i(t)$ , we control the boundaries of topological regime and swap the positions of  $\Gamma_1$  and  $\Gamma_2$ , cf. Fig. 1(a). We split our protocol into six equal time-windows:  $(0, \tau)$  – moving  $\Gamma_1$  to the center of the junction;  $(\tau, 2\tau)$  – moving  $\Gamma_1$  to the edge of vertical chain;  $(2\tau, 3\tau)$  – moving  $\Gamma_2$  to the center of the junction;  $(3\tau, 4\tau)$  – moving  $\Gamma_2$  to the edge of the left chain;  $(4\tau, 5\tau)$  – moving  $\Gamma_1$  to the center of the junction;  $(5\tau, 6\tau)$  – moving  $\Gamma_1$  to the edge of the right chain. These steps are shown explicitly in Fig. 6 presented in the in the Appendix A.

### III. RESULTS

#### A. Geometric phase for a single trijunction

We examine the non-Abelian properties of MZMs by calculating the geometric phases: the Berry phase,  $\phi_{\text{Berry}}$ , in the case of the adiabatic evolution [70] or the Aharonov–Anandan phase,  $\phi_{\text{AA}}$  in the case of a general cyclic evolution [71]. However first, we check when the evolution is cyclic, i.e., when the final quantum state  $|\psi(T)\rangle \langle \psi(T)|$  equals the initial one  $|\psi(0)\rangle \langle \psi(0)|$ , where for the present protocol  $T = 6\tau$ . We examine this property by calculating the loss of the fidelity,

$$w_{\text{loss}} = 1 - |\langle \psi(T) | \psi(0) \rangle|^2, \quad (3)$$

which is shown in Fig. 1(b). One may observe that this quantity decreases when the evolution-time increases and becomes negligible for  $\tau \gtrsim 100$ . The necessary condition for the adiabaticity of the time-evolution is a non-vanishing energy gap between the ground-state and the first excited state. In Fig. 1(c) we show the gap  $\Delta E = \min\{E_1^o - E_0^o, E_1^e - E_0^e\}$  during the entire evolution, where  $E_n^{e(o)}$  is the energy of the  $n$ -eigenstate in the even (odd) parity sector. Since  $\Delta E$  does not vanish, the evolution should be adiabatic for sufficiently large  $\tau$ .

In the case a cyclic evolution the initial and the final wave functions differ only by the phase factor,

$$|\psi(T)\rangle = e^{i\phi} |\psi(0)\rangle = e^{i(\phi_{\text{dyn}} + \phi_{\text{geo}})} |\psi(0)\rangle, \quad (4)$$

which contains both the gauge-invariant geometric phase  $\phi_{\text{geo}}$  and the dynamical phase  $\phi_{\text{dyn}}$  [72]. We evaluate the geometric phase from the standard expression [73],

$$\phi_{\text{geo}} = \arg(\langle \psi(0) | \psi(T) \rangle) - \arg\left(\prod_{j=0}^{N-1} \langle \psi(t_j) | \psi(t_{j+1}) \rangle\right), \quad (5)$$

where  $t_0 = 0$  and  $t_N = T$ . In the case of a generic cyclic quantum evolution,  $\phi_{\text{geo}}$  evaluated from Eq. (5) represents  $\phi_{\text{AA}}$ . Then, the wave function  $|\psi(t_j)\rangle$  is obtained directly from the time-dependent Schrödinger equation. In the case of the adiabatic cyclic evolution,  $\phi_{\text{AA}} = \phi_{\text{Berry}}$ . Then, the wave functions

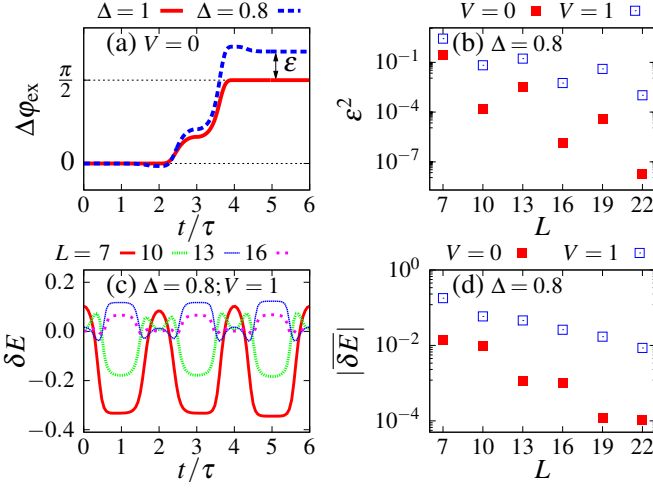


FIG. 2. Single braiding on a single trijunction for  $\mu = 0$ : (a) exchange phase  $\Delta\phi_{\text{ex}}$  during evolution as a function of time  $t/\tau$  for  $L = 7$ ; (b) finite-size scaling of the braiding error  $\epsilon$ ; (c) split between the instantaneous ground-states energies in different parity sectors  $\delta E(t) = E_0^e(t) - E_0^o(t)$ ; (d) finite-size scaling of the average energy split  $\delta E$ .

$|\psi(t_j)\rangle$  are obtained from diagonalization of the instantaneous Hamiltonians  $H(t_j)$ .

The essential quantity for implementing the Majorana quantum gates is the difference between phases acquired during evolution in sectors with even and odd particle numbers:  $\Delta\phi_{\text{geo}} = \phi_{\text{geo}}^e - \phi_{\text{geo}}^o$ , (cf. the basis states of the qubit). As a final test of the adiabatic evolution, in Fig. 1(d) we show that the difference  $\Delta\phi_{\text{AA}} - \Delta\phi_{\text{Berry}}$  decreases with increasing  $\tau$ . The latter difference is significantly larger for systems with many-body interactions, nevertheless one may expect that it vanishes for  $\tau \rightarrow \infty$  also for  $V \neq 0$ . Therefore, from now on we focus only on the adiabatic evolution.

Finally, we introduce the dynamical phase for the adiabatic evolution in the ground-states, e.g. for  $|e_{12}(t)\rangle$ :

$$\phi_{\text{dyn}}^{e,J_{12}} = \int_0^T dt \langle e_{12}(t) | H(t) | e_{12}(t) \rangle, \quad (6)$$

and the phase-difference between even and odd parity sectors,

$$\Delta\phi_{\text{dyn}}^{J_{12}} = \phi_{\text{dyn}}^{e,J_{12}} - \phi_{\text{dyn}}^{o,J_{12}}. \quad (7)$$

The latter quantity is proportional to the difference of the ground-state energies in various sectors,  $\delta E = E_0^e - E_0^o$ . One tries to eliminate the dynamical phase and work only with the geometric phase.

If Majorana fermions are separated in the real-space then they are strict zero-modes, hence  $E_0^e = E_0^o$  and  $\Delta\phi_{\text{dyn}}^{J_{12}} = 0$ . Then, the only contribution to the phase difference comes from the geometric phase,  $\Delta\phi = \Delta\phi_{\text{Berry}}$ . It is well established that the braiding of strict MZMs leads to  $\Delta\phi_{\text{Berry}} = \pm \frac{\pi}{2}$  [45]. In order to construct the phase-gate based on the geometric-phase, one needs a protocol for which  $\Delta\phi_{\text{Berry}} = \pi/4$  [44], whereas  $\Delta\phi_{\text{dyn}} = 0$ . Such gate is unprotected by topology but

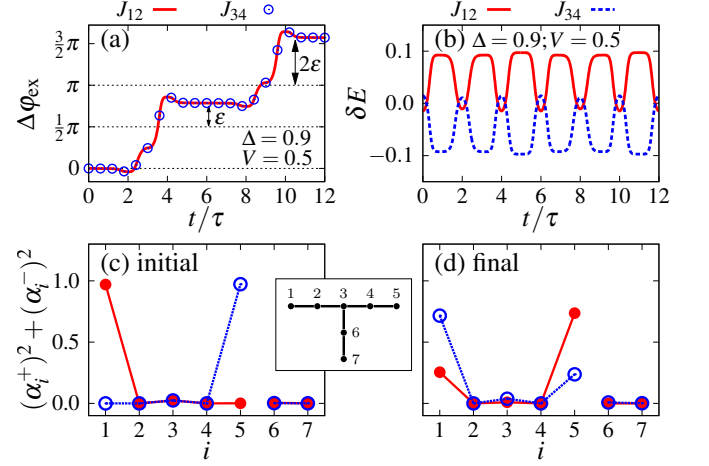


FIG. 3. (a)–(b): Double braiding for  $\mu = 0$ . We set  $\mu_c = 4$  and  $\mu_c = -4$  for the junction  $J_{12}$  and  $J_{34}$ , respectively. (a) exchange phase  $\Delta\phi_{\text{ex}}$  and (b) energy splittings  $\delta E$  determined separately for each junction. Spatial structures of Majorana fermion  $\Gamma_1$  (red solid line) and  $\Gamma_2$  (blue dashed line) (c) before and (d) after single braiding for  $\Delta = 0.8$  and  $V = 0$ . ( $L = 7$ ,  $\mu = 0$ )

it is adiabatic, i.e., the acquired phase is independent of the evolution time.

### B. Braiding error due to overlap of the Majorana fermions

The geometric phase is a gauge-invariant quantity provided that the Hamiltonian follows a closed loop in the parameter space. However, in order to gain more insight, we introduce also the adiabatic *exchange phase*  $\Delta\phi_{\text{ex}}(t)$ , defined for arbitrary  $0 \leq t \leq T$  [53], such that  $\Delta\phi_{\text{Berry}} = \Delta\phi_{\text{ex}}(T)$ . Fig. 2(a) shows the latter quantity. For a special case  $\Delta = 1$ , the MZMs are located on single edge sites and do not overlap during the braiding even for a finite system. Then,  $\Delta\phi_{\text{Berry}} = \frac{\pi}{2}$  for arbitrary  $L$ . However, for  $\Delta \neq 1$  and finite  $L$ , such phase deviates from  $\frac{\pi}{2}$  by a braiding error,  $\epsilon = \Delta\phi_{\text{Berry}} - \frac{\pi}{2}$ . Fig. 2(b) demonstrates that the braiding error is a finite-size effect. In the case of an infinite trijunction, when the MZMs are fully separated in the real space,  $\epsilon$  seems to vanish and the Berry phase equals  $\frac{\pi}{2}$ .

We stress that a non-zero braiding error is intimately connected with a non-vanishing dynamical phase. Overlap of the Majorana fermions lifts the degeneracy of the ground-state,  $E_0^e \neq E_0^o$ , hence in general  $\Delta\phi_{\text{dyn}}^{J_{12}} \neq 0$ . The energy splitting,  $\delta E$ , depends on the distance between the Majorana fermions which varies during the evolution. In Fig. 2(c) we show the instantaneous  $\delta E$  as a function of the evolution time  $t/\tau$  for different system sizes  $L$ . It is clear that  $\delta E$  decreases when  $L$  increases. In order to discuss this effect in more details, we have calculated the average splitting  $\overline{\delta E} = \frac{1}{T} \int_0^T dt \delta E(t)$  which determines also the dynamical phase  $\Delta\phi_{\text{dyn}}^{J_{12}} = T \overline{\delta E}$ . Fig. 2(d) shows the finite-size scaling of  $\overline{\delta E}$  which seems to decay almost exponentially with increasing  $L$ .

### C. Cancellation of the dynamical phases

While the braiding error should be avoided in the topologically protected operations, it may still be very useful for constructing the phase-gate with arbitrary phase-shift. The advantage of such solution over the simplest protocol based on getting Majorana fermions close to each other, consists in that  $\Delta\phi_{\text{Berry}}$  does not depend on the total evolution time  $T$ . However, a non-zero braiding error is intimately connected with a nonzero dynamical phase. Therefore, the idea of using the Berry phase would be useless unless one finds a method of eliminating the dynamical phase. Below we show that  $\Delta\phi_{\text{dyn}}$  can indeed be eliminated by appropriate tuning of junctions which build the Majorana qubit.

We assume that both trijunctions,  $J_{12}$  and  $J_{34}$ , are described by the same Hamiltonian (1) which is particle-hole symmetric up to the term containing  $\mu_i$ , see Eq. (2). Each junction contains *odd* number of sites and the braiding is applied *twice* to each junction. However, one applies positive  $\mu_i$  for one junction and a negative  $\mu_i$  for the other. Namely, the trijunctions  $J_{12}$  and  $J_{34}$  are described, respectively, by the Hamiltonians

$$H_{12}(\Delta_{ij}) = H_0(\Delta_{ij}) + \sum_i \mu_i(t) \tilde{n}_i, \quad (8)$$

$$H_{34}(\Delta_{ij}) = H_0(\Delta_{ij}) - \sum_i \mu_i(t) \tilde{n}_i, \quad (9)$$

where for clarity of the present discussion we explicitly mark the dependence of Hamiltonians on the superconducting order parameter.

In Fig. 3(a) we present the geometric phase,  $\Delta\phi_{\text{ex}}$ , gained by each junction during such double-braiding protocol. The sign of  $\mu_i$  does not influence the geometric phase and we find  $\Delta\phi_{\text{Berry}}^{J_{12}} = \Delta\phi_{\text{Berry}}^{J_{34}} = \pi + 2\varepsilon$ . However, Fig. 3(b) shows that the energy splittings  $\delta E$  for the trijunctions  $J_{12}$  and  $J_{34}$  have opposite signs, hence  $\Delta\phi_{\text{dyn}}^{J_{12}} + \Delta\phi_{\text{dyn}}^{J_{34}} = 0$ . In order to explain the latter identity we assume that the sites within each junction are enumerated according to the scheme shown in the inset in Fig. 3(c). Then, it is easy to check (for odd  $L$ ) that the neighboring sites  $\langle i, j \rangle$  are labeled by integers with opposite parities, i.e., if  $i$  is odd then  $j$  is even. In other words, the trijunctions form a bipartite lattices consisting of two sublattices which contain, respectively, odd and even lattice sites  $i$ .

We consider a standard particle-hole (Shiba) transformation [74],

$$U = (a_L^\dagger - a_L)(a_{L-1}^\dagger + a_{L-1}) \dots (a_2^\dagger + a_2)(a_1^\dagger - a_1), \quad (10)$$

for which  $U^\dagger U = U U^\dagger = 1$  and  $U a_i U^\dagger = (-1)^i a_i^\dagger$ . One finds that Hamiltonians of both junctions are connected via this particle-hole transformation

$$U H_{12}(\Delta_{ij}) U^\dagger = H_{34}(\Delta_{ij}^*), \quad (11)$$

whereas the parity operator

$$P = \prod_{i=1}^L (1 - 2a_i^\dagger a_i) \quad (12)$$

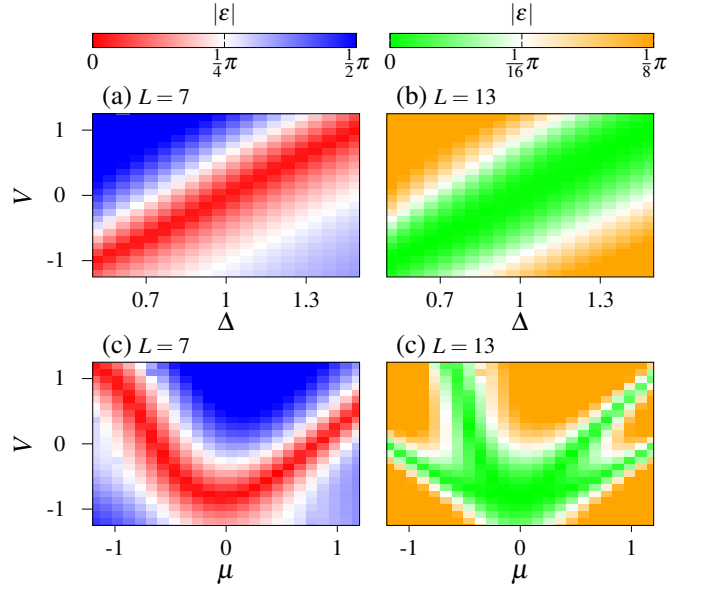


FIG. 4. (color online) Absolute value of the braiding error  $\varepsilon$  (i.e., the deviation of the Berry phase  $\Delta\phi_{\text{Berry}}$  from  $\frac{\pi}{2}$ ): (a)–(b)  $|\varepsilon|$  as a function of interaction  $V$  and superconducting gap  $\Delta$  ( $\mu = 0$ ), for  $L = 7$  and  $L = 13$ , respectively; (c)–(d)  $|\varepsilon|$  as a function of interaction  $V$  and chemical potential  $\mu$  ( $\Delta = 0.6$ ) for  $L = 7$  and  $L = 13$ , respectively.

is odd under the latter transformation,  $U P U^\dagger = (-1)^L P = -P$ . Considering an eigenstate  $|n\rangle$  of  $H_{12}(\Delta_{ij})$ ,

$$H_{12}(\Delta_{ij})|n\rangle = E_n|n\rangle, \quad P|n\rangle = p_n|n\rangle, \quad (13)$$

one finds that  $U|n\rangle$  is an eigenstate of  $H_{34}(\Delta_{ij}^*)$  with energy  $E_n$  but with the opposite parity,  $P U|n\rangle = -p_n U|n\rangle$ . Therefore,  $H_{12}(\Delta_{ij})$  and  $H_{34}(\Delta_{ij}^*)$  have the same energy spectra, however, with swapped parities of the energy levels. It is also clear that the energy spectrum of  $H_{34}(\Delta_{ij}^*)$  is the same as that of  $H_{34}(\Delta_{ij})$ .

Overlap of the Majorana fermions lifts the ground state degeneracy, however the above particle-hole transformation holds true during the entire quantum evolutions. Then, using Eq. (6) one finds that  $\phi_{\text{dyn}}^{e,J_{12}} = \phi_{\text{dyn}}^{o,J_{34}}$  as well as  $\phi_{\text{dyn}}^{o,J_{12}} = \phi_{\text{dyn}}^{e,J_{34}}$  and, consequently,

$$\Delta\phi_{\text{dyn}}^{J_{12}} + \Delta\phi_{\text{dyn}}^{J_{34}} = \phi_{\text{dyn}}^{e,J_{12}} - \phi_{\text{dyn}}^{o,J_{12}} + \phi_{\text{dyn}}^{e,J_{34}} - \phi_{\text{dyn}}^{o,J_{34}} = 0. \quad (14)$$

After the double-braiding protocol, the initial state of the qubit  $|\psi(0)\rangle = |0\rangle + |1\rangle$  will become

$$|\psi(2T)\rangle = \exp(i\chi)(|0\rangle + \exp(4i\varepsilon)|1\rangle), \quad (15)$$

hence the relative phase,  $4\varepsilon$ , is determined solely by the braiding error for the geometric phase.

### D. Tuning of the geometric phase

The main result of the present work concerns the phase-gate based on the braiding error  $\varepsilon$ , i.e., the deviation of the



Berry phase  $\Delta\phi_{\text{Berry}}$  from  $\frac{\pi}{2}$ . The braiding error vanishes for the topologically protected gates when one braids non-overlapping MZMs on an infinite trijunction. However in order to construct the standard  $\pi/8$ -gate, one needs  $\varepsilon = \pi/16$ . Here we show for a finite junction that  $\varepsilon$  may be rather easily tuned via changing the parameters of the Hamiltonian (1).

Since  $\varepsilon$  originates from the overlap of Majorana fermions, it strongly depends on the system size. Fig. 4 shows  $|\varepsilon|$  for  $L = 7$  and  $L = 13$ , which are the smallest system sizes with odd  $L$ . In Figs. 4(a)–4(b) we show how  $|\varepsilon|$  depends on the many-body interaction  $V$  and the superconducting order parameter  $\Delta$  for  $\mu = 0$ . Figs. 4(c)–4(d) show the same quantity for  $\Delta = 0.6$  as a function of the many-body interaction  $V$  and chemical potential  $\mu$ . Tuning the superconducting order parameter or the interaction strength is (most probably) not relevant for realistic experimental setups. Therefore, the most important result is that  $\varepsilon$  may be well tuned via changing the chemical potential.

### E. Spatial structure of overlapping Majorana fermions after braiding

In order to follow the spatial structure of the overlapping Majorana fermions ( $\Gamma_1$  and  $\Gamma_2$ ) during a single adiabatic braiding on a single junction  $J_{12}$ , we represent both fermions as a linear combination of the local Majorana operators  $\gamma_i^+ = a_i + a_i^\dagger$  and  $\gamma_i^- = i(a_i - a_i^\dagger)$ , namely  $\Gamma_m = \sum_i^L (\alpha_i^{m,+} \gamma_i^+ + \alpha_i^{m,-} \gamma_i^-)$  for  $m \in \{1, 2\}$ . Then, we apply the algorithm developed in Ref. [60] to find the coefficients,  $\alpha_i^{m,\pm}$  for each instantaneous Hamiltonian  $H(t)$ . This algorithm targets the MZMs following their formal definition via the commutation relations [6]:  $\{\Gamma_m, \Gamma_{m'}\} = 2\delta_{m,m'}$  and  $[\Gamma_m, H] = 0$ . The latter commutation relations are invariant under the rotation  $\vec{\Gamma} \rightarrow \mathcal{O}(\beta)\vec{\Gamma}$ , where

$$\vec{\Gamma} = \begin{pmatrix} \Gamma_1 \\ \Gamma_2 \end{pmatrix}, \quad \mathcal{O}(\beta) = \begin{pmatrix} \cos\beta & -\sin\beta \\ \sin\beta & \cos\beta \end{pmatrix}, \quad (16)$$

hence also the coefficients,  $\alpha_i^{m,\pm}$ , are defined up to an arbitrary choice of  $\beta$ . Initially at time  $t = t_0$ , we choose the angle  $\beta(t_0)$  following the standard convention in that  $\Gamma_1$  and  $\Gamma_2$  are located at the opposite edges of trijunction, as shown in Fig. 3(c). Then, for each time  $t_j$  during the adiabatic evolution, we find  $\beta(t_j)$  that minimizes the (squared) distance

$$\left\| \vec{\Gamma}(t_j) - \vec{\Gamma}(t_{j-1}) \right\|^2 = \sum_{i=1}^L \sum_{m=1}^2 \sum_{s=\pm} [\alpha_i^{m,s}(t_j) - \alpha_i^{m,s}(t_{j-1})]^2. \quad (17)$$

If Majorana fermions are strict zero-modes then this approach reproduces the standard braiding that swaps the MZMs, i.e.,  $\Gamma_1(T) = \pm\Gamma_2(0)$  and  $\Gamma_2(T) = \mp\Gamma_1(0)$ . The latter swapping may also be written as  $\vec{\Gamma}(T) = \mathcal{O}(\Delta\phi_{\text{Berry}})\vec{\Gamma}(0)$  for  $\Delta\phi_{\text{Berry}} = \pm\frac{\pi}{2}$ . It turns out, that the latter relation holds true also for  $\Delta\phi_{\text{Berry}} \neq \pm\frac{\pi}{2}$ , i.e., also for braiding of the overlapping Majorana fermions. Then however, the cyclic evolution cannot be understood as simple swapping of the Majorana fermions. In particular  $\Gamma_1(T)$  becomes a linear combination of both  $\Gamma_1(0)$

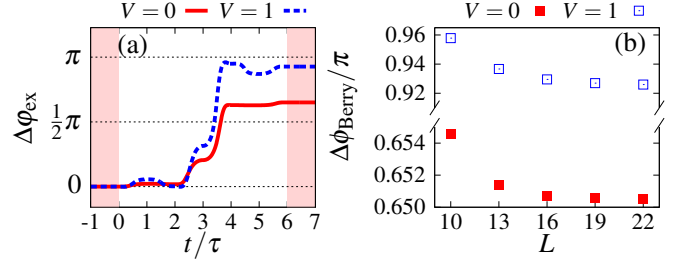


FIG. 5. Braiding of MZMs which are brought together for  $t \in (-\tau, 0)$  and shifted apart for  $t \in (6\tau, 7\tau)$ . We set  $\Delta = 0.8$ ,  $\mu = 0$ . (a) exchange phase  $\Delta\phi_{\text{ex}}$  for  $L = 19$  and  $L' = 7$ . (b) Geometric phase  $\Delta\phi_{\text{Berry}}$  for  $L' = 7$  vs.  $L$ .

and  $\Gamma_2(0)$ , hence it contains non-vanishing contributions located at both edges of the junction, see Figs. 3(c)–3(d). The latter holds true whenever  $\Delta\phi_{\text{Berry}}$  is not a multiple of  $\pm\frac{\pi}{2}$ .

### F. Phase-gate constructed from the braiding error

It is desirable to have a single junction on which one may perform the topologically protected operations, e.g., braiding of separated MZMs with  $\Delta\phi_{\text{Berry}} = \pm\frac{\pi}{2}$ , but also the unprotected adiabatic operations, e.g., the braiding of overlapping MZMs with  $\Delta\phi_{\text{Berry}} \neq \pm\frac{\pi}{2}$ . Due to the former operations, the trijunction with  $L$  sites should be as large as possible. Then, in order to perform the also latter operation, one needs to bring both MZMs towards the center of the junction, so they start to overlap. This may be achieved via appropriate tuning of  $\mu_i(t)$  in the time-window  $t \in (-\tau, 0)$ , see the left shaded area in Fig. 5(a). Then, one may carry out the braiding protocol on the restricted trijunction with  $L' \ll L$  sites in the time-window  $t \in (0, 6\tau)$ . Finally, for  $t \in (6\tau, 7\tau)$  the Majorana fermions are shifted apart to their original positions at the edges of the unrestricted (infinite) junction with  $L$  sites, see the right shaded area in Fig. 5(a).

Fig. 5(a) shows the exchange phase  $\Delta\phi_{\text{ex}}(t)$  for  $L = 19$  and  $L' = 7$ . We note rather negligible changes of  $\Delta\phi_{\text{ex}}(t)$  during the time-windows when MZMs are brought together,  $(-\tau, 0)$ , or when they are shifted apart,  $(6\tau, 7\tau)$ . Fig. 5(b) shows one of main results of the present work: the finite-size scaling of the geometric phase  $\Delta\phi_{\text{Berry}}$  for fixed  $L' = 7$  and various  $L$ . In contrast to results in Fig. 2(a), the braiding error is not a finite-size effect and remains non-zero also for  $L \rightarrow \infty$  provided that  $L'$  is finite and Majorana fermions overlap during the braiding protocol. Weak  $L$ -dependence of  $\Delta\phi_{\text{Berry}}$  in Fig. 5b may originate from the leakage of MZMs into these sites which remain in the trivial regime [13, 75, 76].

## IV. CONCLUSIONS

We have studied the dynamics of a qubit built out of four Majorana quasiparticles evolving on two trijunctions. We focused on a case when Majorana fermions evolve on spatially restricted junctions. Due to their mutual overlapping, they are

not strict zero-modes anymore, hence the qubit acquires both dynamical and geometric phases during the braiding protocol. We have demonstrated that the dynamical contribution may be cancelled out if the trijunctions are described by the same particle-hole symmetric Hamiltonian and contain odd number of the lattice sites. The geometric contribution deviates from that for braiding of strict zero-modes  $\Delta\phi_{\text{Berry}} = \pm\frac{\pi}{2}$ , and the latter deviation allows one to build the adiabatic phase-gate with tunable phase-shift. The only difference with respect to the topologically protected braiding of MZMs consists in that the Majorana fermions are brought together before the braiding and are shifted apart after the braiding. Probably, the protocol still should be followed by some error correction, however the initial error is expected to be smaller than in standard protocol based on the dynamical phase.

### ACKNOWLEDGMENTS

We acknowledge fruitful discussions with A. Ptok and M. Mařka. This work was supported by the National Science Centre, Poland, under Grant No. 2016/23/B/ST3/00647.

### Appendix A: Smooth ramping protocol

We use exactly the same smooth ramping protocol as in Ref. [53]. Fig. 6 illustrates subsequent steps of the braiding protocol and the corresponding time-windows. The swap of MZMs is achieved via appropriate tuning of  $\mu_i(t)$ , see Eqs. (1) and (2) in the main text. Whenever we ramp-up selected sites, we use the following time-dependent function  $g_i(t) \in [0, 1]$ :

$$g_i(t) = m\left(\frac{t}{\tau}[1 + \alpha(\ell - 1)] - \alpha(\ell - i)\right), \quad t \in [0, \tau], \quad (\text{A1})$$

where we take  $\alpha = 0.025$  and  $\ell$  is the length of each chain, i.e.,  $L = 3\ell + 1$ . Here,  $m(x)$  is a scalar function  $m(x) = \sin^2\left(\frac{\pi}{2}r(x)\right)$  and  $r(x)$  is linear ramp  $r(x) = \min[\max(x, 0), 1]$ . For ramp-down protocol, we replace  $t \rightarrow \tau - t$  in Eq. (A1) to reverse the process in time. Fig. 7 shows  $\mu_i(t)$  for the standard braiding protocol relevant for Fig. 2 in the main text. Fig. 8 shows the same but for the extended protocol in which MZMs are first brought together for  $t \in (-\tau, 0)$ , braided for  $t \in (0, 6\tau)$  and shifted apart for  $t \in (6\tau, 7\tau)$ , see Fig. 5 in the main text.

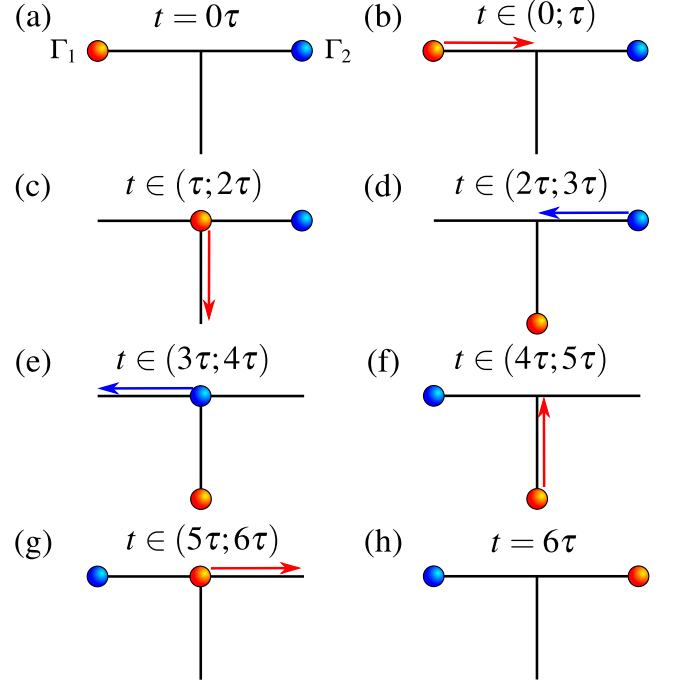


FIG. 6. Braiding protocol: (a) initial position of MZMs; (b) moving  $\Gamma_1$  to the center of the junction; (c) moving  $\Gamma_1$  to the edge of vertical chain; (d) moving  $\Gamma_2$  to the center of the junction; (e) moving  $\Gamma_2$  to the edge of the left chain; (f) moving  $\Gamma_1$  to the center of the junction; (g) moving  $\Gamma_1$  to the edge of the right chain; (h) final position of MZMs.

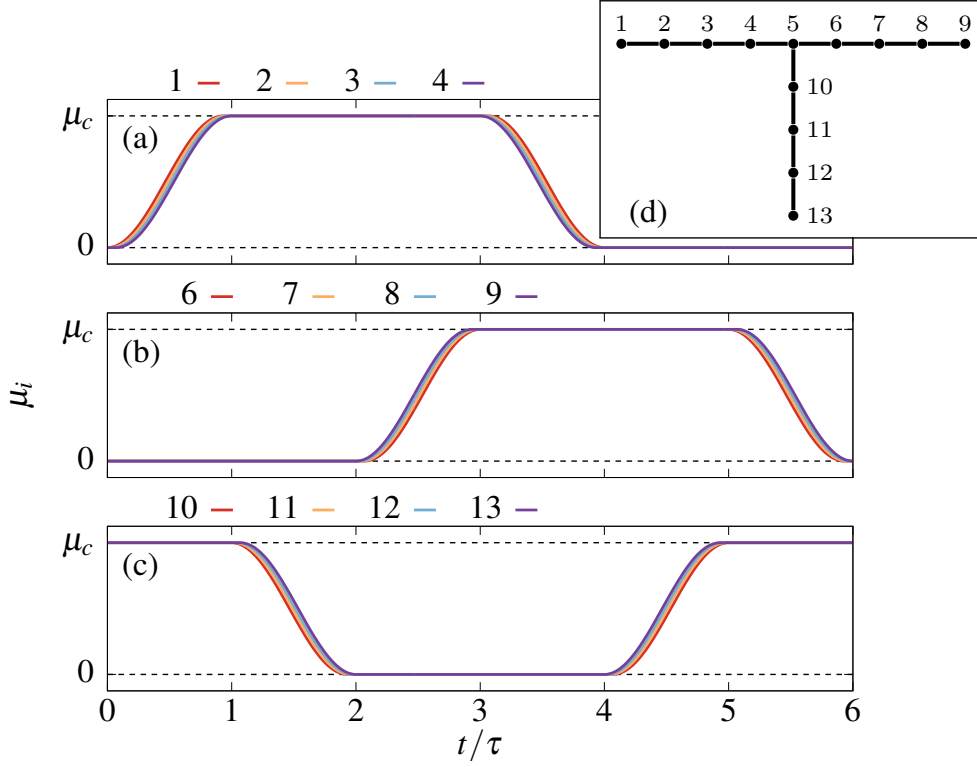


FIG. 7. Standard braiding protocol. (a)–(c) potentials  $\mu_i$  as a function of time  $t/\tau$  in: (a) left (b) right and (c) vertical chain of the trijunction. The numbering of sites is shown in the panel (d).

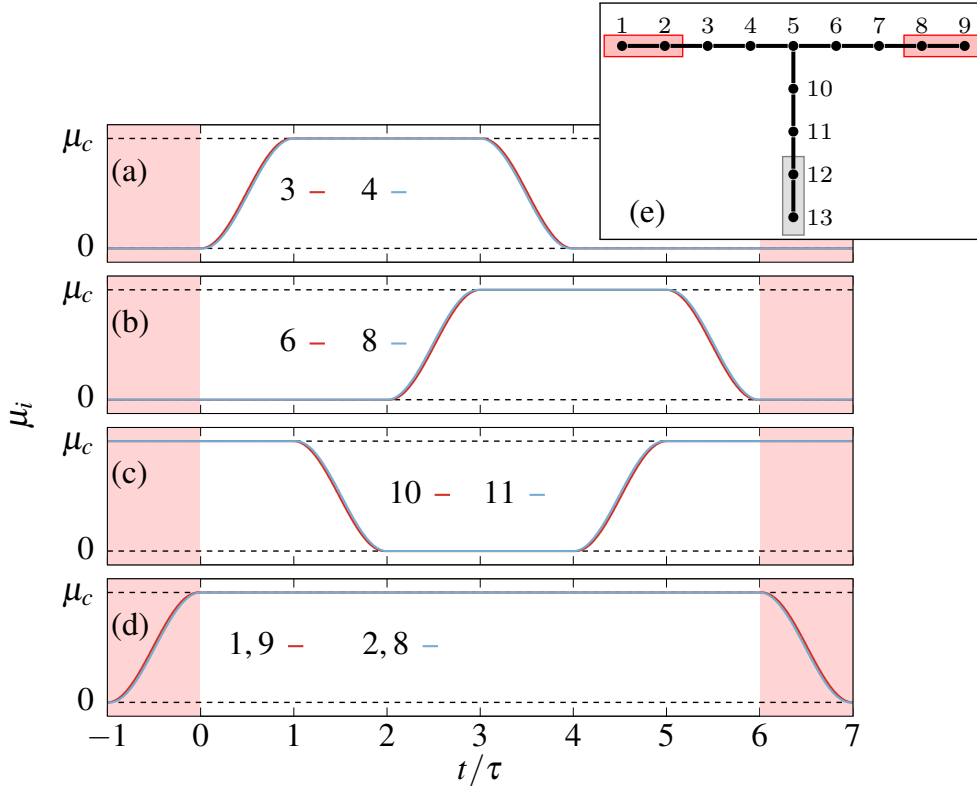


FIG. 8. Extended braiding protocol in which MZMs are brought together for  $t \in (-\tau, 0)$  and shifted apart for  $t \in (6\tau, 7\tau)$ . (a)–(d) potentials  $\mu_i$  as a function of time  $t/\tau$  for selected sites of: (a) left (b) right and (c) vertical chain of the trijunction, which is schematically represented in the panel (e); (d) shows  $\mu_i$  for sites marked with red rectangles in (e). For sites which are marked with gray rectangles in the (e) we set  $\mu_i(t) = \mu_c$  throughout the protocol.

- 
- [1] D. A. Ivanov, “Non-Abelian Statistics of Half-Quantum Vortices in  $p$ -Wave Superconductors,” *Phys. Rev. Lett.* **86**, 268–271 (2001).
- [2] S. Das Sarma, M. Freedman, and C. Nayak, “Topologically Protected Qubits from a Possible Non-Abelian Fractional Quantum Hall State,” *Phys. Rev. Lett.* **94**, 166802 (2005).
- [3] P. Bonderson, M. Freedman, and C. Nayak, “Measurement-Only Topological Quantum Computation,” *Phys. Rev. Lett.* **101**, 010501 (2008).
- [4] C. Nayak, S. H. Simon, A. Stern, M. Freedman, and S. Das Sarma, “Non-Abelian anyons and topological quantum computation,” *Rev. Mod. Phys.* **80**, 1083–1159 (2008).
- [5] A. R. Akhmerov, “Topological quantum computation away from the ground state using Majorana fermions,” *Phys. Rev. B* **82**, 020509(R) (2010).
- [6] S. Das Sarma, M. Freedman, and C. Nayak, “Majorana zero modes and topological quantum computation,” *npj Quantum Inf.* **1**, 15001 (2015).
- [7] S. Plugge, L. A. Landau, E. Sela, A. Altland, K. Flensberg, and R. Egger, “Roadmap to Majorana surface codes,” *Phys. Rev. B* **94**, 174514 (2016).
- [8] D. Aasen, M. Hell, R. V. Mishmash, A. Higginbotham, J. Danon, M. Leijnse, T. S. Jespersen, J. A. Folk, C. M. Marcus, K. Flensberg, and J. Alicea, “Milestones Toward Majorana-Based Quantum Computing,” *Phys. Rev. X* **6**, 031016 (2016).
- [9] T. Karzig, C. Knapp, R. M. Lutchyn, P. Bonderson, M. B. Hastings, C. Nayak, J. Alicea, K. Flensberg, S. Plugge, Y. Oreg, C. M. Marcus, and M. H. Freedman, “Scalable designs for quasiparticle-poisoning-protected topological quantum computation with Majorana zero modes,” *Phys. Rev. B* **95**, 235305 (2017).
- [10] R. Aguado, “Majorana quasiparticles in condensed matter,” *Riv. Nuovo Cim.* **40**, 523 (2017).
- [11] R. M. Lutchyn, E. P. A. M. Bakkers, L. P. Kouwenhoven, P. Krogstrup, C. M. Marcus, and Y. Oreg, “Majorana zero modes in superconductor–semiconductor heterostructures,” *Nat. Rev. Mater.* **3**, 52–68 (2018).
- [12] D. Sticlet, C. Bena, and P. Simon, “Spin and Majorana Polarization in Topological Superconducting Wires,” *Phys. Rev. Lett.* **108**, 096802 (2012).
- [13] A. Ptok, A. Kobińska, and T. Domański, “Controlling the bound states in a quantum-dot hybrid nanowire,” *Phys. Rev. B* **96**, 195430 (2017).
- [14] M. M. Maška and T. Domański, “Polarization of the Majorana quasiparticles in the Rashba chain,” *Sci. Rep.* **7**, 16193 (2017).
- [15] M. M. Maška, A. Gorczyca-Goraj, J. Tworzydło, and T. Domański, “Majorana quasiparticles of an inhomogeneous Rashba chain,” *Phys. Rev. B* **95**, 045429 (2017).
- [16] J. Li, S. Jeon, Y. Xie, A. Yazdani, and B. A. Bernevig, “Majorana spin in magnetic atomic chain systems,” *Phys. Rev. B* **97**, 125119 (2018).
- [17] A. Kobińska, T. Domański, and A. Ptok, “Delocalisation of Majorana quasiparticles in plaquette–nanowire hybrid system,” (2018), [arXiv:1808.05281](https://arxiv.org/abs/1808.05281).
- [18] A. Kobińska and A. Ptok, “Electrostatic formation of the Majorana quasiparticles in the quantum dot–nanoring structure,” *J. Phys. Condens. Matter* **31**, 185302 (2019).
- [19] C.-X. Liu, J. D. Sau, T. D. Stanescu, and S. Das Sarma, “Andreev bound states versus Majorana bound states in quantum dot–nanowire–superconductor hybrid structures: Trivial versus topological zero-bias conductance peaks,” *Phys. Rev. B* **96**, 075161 (2017).
- [20] C.-X. Liu, J. D. Sau, and S. Das Sarma, “Distinguishing topological Majorana bound states from trivial Andreev bound states: Proposed tests through differential tunneling conductance spectroscopy,” *Phys. Rev. B* **97**, 214502 (2018).
- [21] M. Hell, K. Flensberg, and M. Leijnse, “Distinguishing Majorana bound states from localized Andreev bound states by interferometry,” *Phys. Rev. B* **97**, 161401(R) (2018).
- [22] M. T. Deng, C. L. Yu, G. Y. Huang, M. Larsson, P. Caroff, and H. Q. Xu, “Anomalous zero-bias conductance peak in a Nb–InSb nanowire–Nb hybrid device,” *Nano Lett.* **12**, 6414 (2012).
- [23] V. Mourik, K. Zuo, S. M. Frolov, S. R. Plissard, E. P. A. M. Bakkers, and L. P. Kouwenhoven, “Signatures of Majorana fermions in hybrid superconductor–semiconductor nanowire devices,” *Science* **336**, 1003 (2012).
- [24] A. Das, Y. Ronen, Y. Most, Y. Oreg, M. Heiblum, and H. Shtrikman, “Zero-bias peaks and splitting in an Al–InAs nanowire topological superconductor as a signature of Majorana fermions,” *Nat. Phys.* **8**, 887 (2012).
- [25] A. D. K. Finck, D. J. Van Harlingen, P. K. Mohseni, K. Jung, and X. Li, “Anomalous Modulation of a Zero-Bias Peak in a Hybrid Nanowire–Superconductor Device,” *Phys. Rev. Lett.* **110**, 126406 (2013).
- [26] F. Nichele, A. C. C. Drachmann, A. M. Whiticar, E. C. T. O’Farrell, H. J. Suominen, A. Fornieri, T. Wang, G. C. Gardner, C. Thomas, A. T. Hatke, P. Krogstrup, M. J. Manfra, K. Flensberg, and C. M. Marcus, “Scaling of Majorana zero-bias conductance peaks,” *Phys. Rev. Lett.* **119**, 136803 (2017).
- [27] Ö. Gül, H. Zhang, J. D. S. Bommer, M. W. A. de Moor, D. Car, S. R. Plissard, E. P. A. M. Bakkers, A. Geresdi, K. Watanabe, T. Taniguchi, and L. P. Kouwenhoven, “Ballistic Majorana nanowire devices,” *Nat. Nanotech.* **13**, 192 (2018).
- [28] M. T. Deng, S. Vaitiekėnas, E. B. Hansen, J. Danon, M. Leijnse, K. Flensberg, J. Nygård, P. Krogstrup, and C. M. Marcus, “Majorana bound state in a coupled quantum-dot hybrid–nanowire system,” *Science* **354**, 1557 (2016).
- [29] M.-T. Deng, S. Vaitiekėnas, E. Prada, P. San-Jose, J. Nygård, P. Krogstrup, R. Aguado, and C. M. Marcus, “Nonlocality of majorana modes in hybrid nanowires,” *Phys. Rev. B* **98**, 085125 (2018).
- [30] H. Zhang, C.-X. Liu, S. Gazibegovic, D. Xu, J. A. Logan, G. Wang, N. Van Loo, J. D. Bommer, M. W. De Moor, D. Car, *et al.*, “Quantized majorana conductance,” *Nature* **556**, 74 (2018).
- [31] D. Wang, L. Kong, P. Fan, H. Chen, S. Zhu, W. Liu, L. Cao, Y. Sun, S. Du, J. Schneeloch, R. Zhong, G. Gu, L. Fu, H. Ding, and H.-J. Gao, “Evidence for Majorana bound states in an iron-based superconductor,” *Science* **362**, 333–335 (2018).
- [32] S. Nadj-Perge, I. K. Drozdov, J. Li, H. Chen, S. Jeon, J. Seo, A. H. MacDonald, B. A. Bernevig, and A. Yazdani, “Observation of Majorana fermions in ferromagnetic atomic chains on a superconductor,” *Science* **346**, 602 (2014).
- [33] R. Pawlak, M. Kisiel, J. Klinovaja, T. Meier, S. Kawai, T. Glatzel, D. Loss, and E. Meyer, “Probing atomic structure and Majorana wavefunctions in mono-atomic Fe chains on superconducting Pb surface,” *npj Quantum Inf.* **2**, 16035 (2016).
- [34] B. E. Feldman, M. T. Randeria, J. Li, S. Jeon, Y. Xie, Z. Wang, I. K. Drozdov, B. A. Bernevig, and A. Yazdani, “High-resolution studies of the Majorana atomic chain platform,” *Nat. Phys.* **13**, 286 (2016).



- [35] M. Ruby, B. W. Heinrich, Y. Peng, F. von Oppen, and K. J. Franke, "Exploring a proximity-coupled Co chain on Pb(110) as a possible Majorana platform," *Nano Lett.* **17**, 4473 (2017).
- [36] S. Jeon, Y. Xie, J. Li, Z. Wang, B. A. Bernevig, and A. Yazdani, "Distinguishing a Majorana zero mode using spin-resolved measurements," *Science* **358**, 772 (2017).
- [37] H. Kim, A. Palacio-Morales, T. Posske, L. Rózsa, K. Palotás, L. Szunyogh, M. Thorwart, and R. Wiesendanger, "Toward tailoring Majorana bound states in artificially constructed magnetic atom chains on elemental superconductors," *Sci. Adv.* **4**, eaar5251 (2018).
- [38] H.-H. Sun and J.-F. Jia, "Detection of Majorana zero mode in the vortex," *npj Quant. Mater.* **2**, 34 (2017).
- [39] T. Machida, Y. Sun, S. Pyon, S. Takeda, Y. Kohsaka, T. Hanaguri, T. Sasagawa, and T. Tamegai, "Zero-energy vortex bound state in the superconducting topological surface state of Fe(Se,Te)," *Nat. Mater.* **18**, 811–815 (2019).
- [40] K. Jiang, X. Dai, and Z. Wang, "Quantum Anomalous Vortex and Majorana Zero Mode in Iron-Based Superconductor Fe(Te,Se)," *Phys. Rev. X* **9**, 011033 (2019).
- [41] C.-K. Chiu, T. Machida, Y. Huang, T. Hanaguri, and F.-C. Zhang, "Scalable Majorana vortex modes in iron-based superconductors," (2019), [arXiv:1904.13374](https://arxiv.org/abs/1904.13374).
- [42] G. C. Ménard, S. Guissart, C. Brun, R. T. Leriche, M. Trif, F. Debontridder, D. Demaille, D. Roditchev, P. Simon, and T. Cren, "Two-dimensional topological superconductivity in Pb/Co/Si(111)," *Nat. Commun.* **8**, 2040 (2017).
- [43] A. Palacio-Morales, E. Mascot, S. Cocklin, H. Kim, S. Rachel, D. K. Morr, and R. Wiesendanger, "Atomic-Scale Interface Engineering of Majorana Edge Modes in a 2D Magnet-Superconductor Hybrid System," (2018), [arXiv:1809.04503](https://arxiv.org/abs/1809.04503).
- [44] M. A. Nielsen and I. L. Chuang, *Quantum Computation and Quantum Information: 10th Anniversary Edition*, 10th ed. (Cambridge University Press, New York, NY, USA, 2011).
- [45] J. Alicea, Y. Oreg, G. Refael, F. Von Oppen, and M. P. Fisher, "Non-Abelian statistics and topological quantum information processing in 1D wire networks," *Nat. Phys.* **7**, 412 (2011).
- [46] B. van Heck, A. R. Akhmerov, F. Hassler, M. Burrello, and C. W. J. Beenakker, "Coulomb-assisted braiding of Majorana fermions in a Josephson junction array," *New J. Phys.* **14**, 035019 (2012).
- [47] T. Karzig, Y. Oreg, G. Refael, and M. H. Freedman, "Universal Geometric Path to a Robust Majorana Magic Gate," *Phys. Rev. X* **6**, 031019 (2016).
- [48] L.-H. Wu, Q.-F. Liang, and X. Hu, "New scheme for braiding Majorana fermions," *Sci. Technol. Adv. Mater.* **15**, 064402 (2014).
- [49] F. L. Pedrocchi and D. P. DiVincenzo, "Majorana Braiding with Thermal Noise," *Phys. Rev. Lett.* **115**, 120402 (2015).
- [50] Q.-B. Cheng, J. He, and S.-P. Kou, "Verifying non-Abelian statistics by numerical braiding Majorana fermions," *Phys. Lett. A* **380**, 779–782 (2016).
- [51] J. Li, T. Neupert, B. A. Bernevig, and A. Yazdani, "Manipulating Majorana zero modes on atomic rings with an external magnetic field," *Nat. Commun.* **7**, 10395 (2016).
- [52] A. Matos-Abiad, J. Shabani, A. D. Kent, G. L. Fatin, B. Scharf, and I. Žutić, "Tunable magnetic textures: From Majorana bound states to braiding," *Solid State Commun.* **262**, 1–6 (2017).
- [53] M. Sekania, S. Plugge, M. Greiter, R. Thomale, and P. Schmitteckert, "Braiding errors in interacting Majorana quantum wires," *Phys. Rev. B* **96**, 094307 (2017).
- [54] B. Bauer, T. Karzig, R. V. Mishmash, A. E. Antipov, and J. Alicea, "Dynamics of Majorana-based qubits operated with an array of tunable gates," *SciPost Phys.* **5**, 4 (2018).
- [55] K. Ritland and A. Rahmani, "Optimal noise-canceling shortcuts to adiabaticity: application to noisy Majorana-based gates," *New J. Phys.* **20**, 065005 (2018).
- [56] C. Malciu, L. Mazza, and C. Mora, "Braiding Majorana zero modes using quantum dots," *Phys. Rev. B* **98**, 165426 (2018).
- [57] S. Bravyi and A. Kitaev, "Universal quantum computation with ideal Clifford gates and noisy ancillas," *Phys. Rev. A* **71**, 022316 (2005).
- [58] A. Y. Kitaev, "Unpaired Majorana fermions in quantum wires," *Phys. Usp.* **44**, 131 (2001).
- [59] R. Thomale, S. Rachel, and P. Schmitteckert, "Tunneling spectra simulation of interacting Majorana wires," *Phys. Rev. B* **88**, 161103(R) (2013).
- [60] A. Więckowski, M. M. Maška, and M. Mierzejewski, "Identification of Majorana Modes in Interacting Systems by Local Integrals of Motion," *Phys. Rev. Lett.* **120**, 040504 (2018).
- [61] E. M. Stoudenmire, J. Alicea, O. A. Starykh, and M. P. A. Fisher, "Interaction effects in topological superconducting wires supporting Majorana fermions," *Phys. Rev. B* **84**, 014503 (2011).
- [62] F. Hassler and D. Schuricht, "Strongly interacting Majorana modes in an array of Josephson junctions," *New J. Phys.* **14**, 125018 (2012).
- [63] Y. Peng, F. Pientka, L. I. Glazman, and F. von Oppen, "Strong Localization of Majorana End States in Chains of Magnetic Adatoms," *Phys. Rev. Lett.* **114**, 106801 (2015).
- [64] N. M. Gergs, L. Fritz, and D. Schuricht, "Topological order in the Kitaev/Majorana chain in the presence of disorder and interactions," *Phys. Rev. B* **93**, 075129 (2016).
- [65] F. Domínguez, J. Cayao, P. San-Jose, R. Aguado, A. L. Yeyati, and E. Prada, "Zero-energy pinning from interactions in Majorana nanowires," *npj Quantum Mater.* **2**, 13 (2017).
- [66] J. Alicea, "New directions in the pursuit of Majorana fermions in solid state systems," *Rep. Prog. Phys.* **75**, 076501 (2012).
- [67] H. Katsura, D. Schuricht, and M. Takahashi, "Exact ground states and topological order in interacting Kitaev/Majorana chains," *Phys. Rev. B* **92**, 115137 (2015).
- [68] H. Fehske, J. Schleede, G. Schubert, G. Wellein, V. S. Filinov, and A. R. Bishop, "Numerical approaches to time evolution of complex quantum systems," *Phys. Lett. A* **373**, 2182 – 2188 (2009).
- [69] G. Torres-Vega, "Chebyshev scheme for the propagation of quantum wave functions in phase space," *J. Chem. Phys.* **99**, 1824–1827 (1993).
- [70] M. V. Berry, "Quantal phase factors accompanying adiabatic changes," *Proc. Roy. Soc. Lond. A* **392**, 45–47 (1983).
- [71] Y. Aharonov and J. Anandan, "Phase change during a cyclic quantum evolution," *Phys. Rev. Lett.* **58**, 1593–1596 (1987).
- [72] J. Anandan, J. Christian, and K. Wanelik, "Resource Letter GPP-1: Geometric Phases in Physics," *Am. J. Phys.* **65**, 180–185 (1997).
- [73] N. Mukunda and R. Simon, "Quantum Kinematic Approach to the Geometric Phase. I. General Formalism," *Ann. Phys.* **228**, 205–268 (1993).
- [74] F. H. L. Essler, H. Frahm, F. Göhmann, A. Klümper, and V. E. Korepin, *The One-Dimensional Hubbard Model* (Cambridge University Press, 2005).
- [75] J. Klinovaja and D. Loss, "Composite majorana fermion wave functions in nanowires," *Phys. Rev. B* **86**, 085408 (2012).
- [76] D. A. Ruiz-Tijerina, E. Vernek, L. G. G. V. Dias da Silva, and J. C. Egues, "Interaction effects on a majorana zero mode leaking into a quantum dot," *Phys. Rev. B* **91**, 115435 (2015).